Test of Halperin-Lubensky-Ma crossover function at the *N*–Sm-*A* transition in liquid crystal binary mixtures via high-resolution birefringence measurements

Sevtap Yıldız,* Mehmet Can Çetinkaya, Şenay Üstünel, and Haluk Özbek
Department of Physics, Istanbul Technical University, 34469 Maslak, Istanbul, Turkey

Jan Thoen†
Soft Matter and Biophysics, Department of Physics and Astronomy, KU Leuven, 3001 Leuven, Belgium
(Received 5 April 2016; published 27 June 2016)

We report optical birefringence data for a series of mixtures of the liquid crystals octylcyanobiphenyl (8CB) and decylcyanobiphenyl (10CB). Nematic order parameter S data in the nematic and smectic A phases have been derived from phase angle changes obtained in temperature scans with a rotating analyzer method. These S values have been used to arrive at values for possible entropy discontinuities at the smectic A to nematic phase transition temperature T_{NA}. The 10CB mole fraction dependence of the obtained entropy discontinuities could be well fitted with a crossover function consistent with the mean-field free-energy expression with a nonzero cubic term arising from the coupling between the smectic-A order parameter and the orientational order parameter director fluctuations in the Halperin-Lubensky-Ma theory. The obtained results are in good agreement with existing results from adiabatic scanning calorimetry. By exploiting the fact that the temperature derivative of the order parameter $S(T)$ near T_{NA} exhibits the same power law divergence as the specific heat capacity, we have extracted the effective critical exponent α values for the compositions under study. The critical exponent α has been observed to reach the tricritical value $\alpha_{\mathrm{TCP}} = 0.5$ for the 10CB mole fraction of $x = 0.330$.

DOI: 10.1103/PhysRevE.93.062706

I. INTRODUCTION

Thermotropic liquid crystals (LCs) are large anisotropic organic molecules, known to exhibit intermediate phases, namely, mesophases, which differ from each other in their degree of order and symmetry. Two of the most common mesophases located between an isotropic liquid and a crystalline solid are the orientationally ordered nematic (N) and the layered smectic (Sm) phases. Within the N phase, long-range orientational order of the long molecular axes along the director is observed without any long-range positional order, while in the smectic A (SmA) phase, one-dimensional positional order in the form of layers, with the layer normal along the director, occurs [1–3].

To date various types of phase transitions seen in liquid crystalline materials have been subjects of intensive studies in an effort to test the general concepts of phase transitions and critical phenomena in soft matter physics. Among these transitions, the nematic-smectic-A (N-SmA) transition has been the most exhaustively studied one, but it is still not fully understood [4–7]. Although the N-SmA transition is expected to fall into the three-dimensional XY universality class (3D XY) [1–3], the experimental results to date have not shown a clear case of 3D XY universality, since the situation is quite complicated due to coupling between the order parameters and their fluctuations. Experimentally, nonuniversal effective critical exponents and anisotropic correlation length divergences have been reported [6]. Based on mean-field molecular and phenomenological theories, the N-SmA transition has been shown to crossover from second order in nature to first order through a tricritical point owing to the coupling between the nematic and the smectic-A order parameters (Ψ) [1,8,9]. The N-SmA transition is of second order for a wide N range (weak coupling), while a narrow N range (strong coupling) yields a first-order N-SmA transition. Later, Halperin, Lubensky, and Ma (HLM), by taking into account the coupling between the SmA-order parameter and the nematic director fluctuations, proposed that the N-SmA transition should be weakly first order even if there is no measurable latent heat [10]. The HLM discontinuity is expected to be weak and to decrease with increasing width the nematic range, but never vanishes. Subsequently, Anisimov *et al.* [11,12] pointed out that this coupling generates a cubic term, i.e., a $|\Psi|^3$ term, in the effective free energy expansion in the smectic order parameter Ψ, which ensures the N-SmA transition to be first order [11,12]. They also derived a universal crossover form (universal scaling form) of the latent heat [see Eq. (20) in Ref. [12]], which is itself consistent with the HLM predictions as well. In Ref. [12], the authors, by reanalyzing the published latent heat data of several LC mixtures [13–15], tested successfully the validity of this crossover form. A good description of the experimental data was obtained.

Of particular relevance has been the case of the pure 8CB (octylcyanobiphenyl) LC since the N-SmA transition in pure 8CB was expected to be of first order on the basis of the above analysis by Anisimov *et al.* [12]. For the N-Sm A transition, the derived values for the latent heat (or corresponding entropy discontinuity) of pure 8CB, on the basis of the optical experiments [16–19], substantially deviated from the upper limit set by adiabatic scanning calorimetry (ASC) measurements [5] and from the predicted HLM value [12,20,21]. In a recent work [22] we have resolved this discrepancy related to pure 8CB via high-resolution optical birefringence measurements. We showed that, within the resolution of our experiments, the N-SmA transition is continuous, and a possible discontinuity in the nematic order parameter $S(T)$ at the N-SmA transition,

*Corresponding author: sevtap@itu.edu.tr
†Corresponding author: jan.thoen@fys.kuleuven.be

T_{NA} is smaller than the other estimates found in literature and consistent with the value derived from ASC measurements and with the HLM predictions as well.

Regarding the Halperin-Lubensky-Ma effect [10] and the validity of a crossover form of the entropy discontinuity at the *N*-Sm*A* transition significant experimental evidence seems, as already pointed out, to be available. This experimental evidence is, however, largely based on high-resolution calorimetry in liquid crystalline mixtures. Binary mixtures of compounds of the alkylcyanobiphenyl (*n*CB) and alkyloxycyanobiphenyl (*n*OCB) homologous series have mainly been studied, in particular 8CB+10CB [14], 9CB+10CB [13,14], and 8OCB+9OCB [20,23]. Calorimetric results have been obtained for mixtures of $\overline{6}\mathrm{O}\overline{10} + \overline{6}\mathrm{O}\overline{12}$ of the alkyloxyphenyl-alkyloxybenzoate homologous series [15] and for mixtures of 4O.8+6O.8 of alkyloxybenzylidene-alkylaniline [23] as well. Recently mixtures of the LC heptyloxybiphenyl with the nonmesogenic compound heptane (7OCB+heptane) also have been studied calorimetrically [21]. All these calorimetric results confirm the existence of the HLM effect and consistency with the universal crossover form. Experimental investigations with other techniques are very limited. The system of 8CB+10CB has also been measured by Tamblyn *et al.* [24] via capillary-length measurements, and by Yethiraj *et al.* via an intensity fluctuation microscopic technique [16–18]. Tamblyn *et al.* confirmed the validity of the calorimetrically derived crossover form for the latent heat. Yethiraj *et al.* reported that derived values for the entropy discontinuity are in good accordance with the HLM predictions for 10CB concentrations where the *N* range is very small, whereas for lower 10CB concentrations, closer to pure 8CB, with larger *N* ranges, there was a systematic deviation from the calorimetric results and the HLM predictions (see Fig. 2 in Ref. [17] and Fig. 11 in Ref. [18]).

In view of the above, there seems to be a need to test the calorimetric conclusions by additional measurements with other high-resolution techniques. Such a technique is our rotating-analyzer birefringence technique, which has been proven to produce very high-resolution results for two different pure LC compounds exhibiting a smectic *A* to nematic phase transition. These compounds are partially bilayer polar 8CB [22] and the monolayer nonpolar $\overline{10}\mathrm{O}\overline{4}$ (butyloxyphenyl-decyloxybenzoate) [25]. Because of the contradicting results between the calorimetric data and the results of the optical fluctuation microscopy data for binary system 8CB+10CB we think it is important to apply our birefringence methods to this system to arrive at an alternative test. In this way we would also demonstrate that our technique works not only for pure LCs but for mixtures as well.

II. THEORETICAL BACKGROUND

In order to derive the nematic (orientational) order parameter $S(T)$ from the optical birefringence $\Delta n(T)$ the isotropic internal field model by Vuks, Chandrasekhar, and Madhusudana (VCM model) [26] has been widely used [22,25,27–30]. According to the VCM model the relation between $S(T)$ and the refractive indices and birefringence, $\Delta n = n_e - n_0$ is given by

$$\frac{\Delta\sigma}{\langle\sigma\rangle}S(T) = \frac{(n_e + n_0)\Delta n}{\langle n^2\rangle - 1}, \tag{1}$$

where $\langle n^2\rangle = (n_e^2 + 2n_0^2)/3$, $\Delta\sigma = \sigma_l - \sigma_t$, and $\langle\sigma\rangle = (\sigma_l + 2\sigma_t)/3$ with σ_l and σ_t longitudinal and transverse polarizabilities relative to the long molecular axis, respectively. As we discussed in our previous works [22,25], under the approximations $(n_e + n_0)/2 \approx n_I$ and $\langle n^2\rangle \approx n_I^2$, with n_I the value of the refractive index in the isotropic phase just above the *N*-*I* transition temperature T_{IN}, Eq. (1) can be rewritten as

$$\frac{\Delta\sigma}{\langle\sigma\rangle}S(T) = \frac{2n_I\Delta n}{n_I^2 - 1}. \tag{2}$$

Moreover, the temperature behavior of $S(T)$ has been shown to be well described by a four-parameter power-law expression [31–33], which is in accord with the weakly first-order character of the *N*-*I* transition (nonzero cubic invariant) [8,9,34]. Together with the fact that the nematic order would become perfect at $T = 0$ *K*, the temperature behavior of Δn can be given as

$$\Delta n = \frac{n_I^2 - 1}{2n_I}\frac{\Delta\sigma}{\langle\sigma\rangle}\left[S^{**} + (1 - S^{**})\left|1 - \frac{T}{T^{**}}\right|^{\beta}\right], \tag{3}$$

where T^{**} is the effective second-order transition temperature seen from below the *N*-*I* transition temperature T_{IN}, β is the critical exponent, and S^{**} is the order parameter at $T = T^{**}$. It seen that the coefficient in front of the square bracket in Eq. (3) can be written as a new constant $\Delta n_0 = \frac{n_I^2-1}{2n_I}\frac{\Delta\sigma}{\langle\sigma\rangle}$. Thus Eq. (3) reads

$$\Delta n = \Delta n_0\left[S^{**} + (1 - S^{**})\left|1 - \frac{T}{T^{**}}\right|^{\beta}\right]. \tag{4}$$

One can see that at $T = 0$ *K*, $\Delta n(T = 0\ K) = \Delta n_0$ and that it is consistent with the scaling condition $S(T = 0\ K) = 1$ [22,25,31,32]. Hence one can infer that, within very good accuracy, the other parameter $S(T)$ can be deduced directly from $\Delta n(T)$ data via the relation

$$S(T) = \frac{\Delta n(T)}{\Delta n_0} \tag{5}$$

without addressing the n_I value, and with Δn_0 the hypothetical birefringence at $T = 0$ *K* [35,36]. In order to further check the validity of Eq. (5), for pure 8CB, we have used the fit result presented in Ref. [35], $\Delta n_0 = 0.3204$; also by using $n_I = 1.5655$ [31] we obtained $\frac{\Delta\sigma}{\langle\sigma\rangle} = 0.6914$ with the help of $\Delta n_0 = \frac{n_I^2-1}{2n_I}\frac{\Delta\sigma}{\langle\sigma\rangle}$. Notice that this value (for the wavelength of 633 nm) is in good agreement with the value $\frac{\Delta\sigma}{\langle\sigma\rangle} = 0.674$ given in Table 3 of Ref. [31] (for a wavelength of 589 nm) and with the value we reported in Ref. [22]. By using the value $\Delta n_0 = 0.3204$ one can obtain $S(T) = \frac{\Delta n(T)}{0.3204} = 3.121\Delta n(T)$, being in good agreement with Eq. (2) reported in Ref. [22]. As will be discussed below, Eq. (5) will be used in deriving the entropy discontinuity near the *N*-Sm*A* transition from the order parameter $S(T)$.

In the framework of the HLM theory, the effective Landau free energy of the Sm*A* phase can be written as [12]

$$F = F_N + \tfrac{1}{2}\alpha_0(T - T_0)|\Psi|^2 - \tfrac{1}{3}B|\Psi|^3 + \tfrac{1}{4}C|\Psi|^4 + \tfrac{1}{6}D|\Psi|^6, \quad (6)$$

where F_N is the free energy in the N phase and $|\Psi|$ the smectic-A order parameter. The temperature T_0 is different from the N-SmA transition temperature T_{NA} and $B > 0$, $D > 0$. In the N phase, above T_{NA}, the only term in the free energy F is F_N, since $|\Psi|$ is zero. Notice that the director $\hat{n}$ is not fixed in a direction perpendicular to the smectic layers and it fluctuates about this direction. This fluctuation is coupled to the smectic order parameter and thus results in a quite small cubic term [see Eq. (6)], which makes the transition weakly first order [12]. Moreover, it is a well-known fact that since orientational fluctuations are suppressed in the Sm*A* phase, the smectic ordering is intrinsically coupled with an enhancement in the nematic ordering. This coupling, the so-called deGennes-McMillan coupling [8,9], appears as renormalization of the coefficient of the $|\Psi|^4$ term. The point at which the coefficient C in Eq. (6) vanishes is known as the Landau tricritical point (LTP), where the transition is driven from first order to second order in nature. For binary LC mixtures the variation of the $|\Psi|^4$ term near the LTP is modeled by $C = C_0(x - x^*)$ with $C_0 < 0$ and x the mole fraction in the mixture. Notice that at the LTP, i.e., at the mole fraction x^*, one has $C = 0$. It is straightforward to show that the entropy discontinuity at the LTP can be written as [12]

$$\frac{\Delta\bar{S}}{R} = \frac{1}{2}\alpha_0\left(\frac{B}{2D}\right)^{\frac{2}{3}}, \quad (7)$$

where R is the gas constant. Here $\bar{S}$ represents the entropy and should not be confused with the nematic order parameter S. Further, Anisimov *et al.* [12] derived a universal scaling (crossover) form between the reduced entropy difference $\bar{s} \equiv \frac{\Delta\bar{S}}{R}$ and the mole fraction x, which is given by

$$\frac{\bar{s}}{\bar{s}^*} - \left(\frac{\bar{s}}{\bar{s}^*}\right)^{-\frac{1}{2}} = \frac{\hat{a}}{\bar{s}^*}(x - x^*) \equiv y - y^*, \quad (8)$$

where $\hat{a} = -\frac{3}{8}(\frac{\alpha_0 C_0}{D})$ and $\bar{s}^* \equiv \frac{\Delta\bar{S}^*}{R}$. Also notice that $y \equiv \frac{\hat{a}x}{\bar{s}}$ and $y^* \equiv \frac{\hat{a}x}{\bar{s}^*}$. Furthermore, in the vicinity of the N-I transition the nematic free energy F_N is given by

$$F_N = F_I + \tfrac{1}{2}a(T - T^*)S^2 + \tfrac{1}{3}bS^3 + \tfrac{1}{4}cS^4, \quad (9)$$

where F_I is the free energy in the isotropic phase, T^* is the stability limit of the isotropic phase, and the constants a and $c > 0$ and $b < 0$. The presence of the cubic term makes the N-I transition first order at T_{IN} with a finite discontinuity $S_{IN} = \frac{2b}{3c}$ in the nematic order parameter S. In our previous work [22], by inserting F_N [Eq. (9)] in F (Eq. (6)], we derived an expression for the entropy change $\Delta\bar{S}$ in terms of the order parameter change ΔS_{NA} in the vicinity of the N-SmA transition, which is given by

$$\Delta\bar{S} = aS_{NA}\Delta S_{NA} \quad (10)$$

with $S_{NA} = \frac{[S_A(T_{NA}) + S_N(T_{NA})]}{2}$ and $\Delta S_{NA}(T_{NA}) = S_A - S_N$. The value of the parameter a can be evaluated at the N-I transition using the relation

$$a = \frac{2(\Delta H_{IN})}{T_{IN}S_{IN}^2} \quad (11)$$

with ΔH_{IN} the latent heat of the N-I transition, which can be obtained via ASC measurements [5]. Further details of the derivation can be found in Ref. [22]. In Table I we give the a values of Eq. (11) and the values of the quantities to calculate the a values. In Ref. [22] we also discussed the validity of Eq. (10) in the framework of the HLM theory. In this work, for 8CB-10CB binary mixtures, we have tested the scaling form in Eq. (8) by deriving $\bar{s} \equiv \frac{\Delta\bar{S}}{R}$ from $\Delta n(T)$ data using the relations Eqs. (10)–(11) and have compared the results with the previously published values.

TABLE I. Values of the parameter a of Eq. (11) and the values of quantities used to derive it. The first row is quoted from Ref. [22].

x	$\Delta H_{IN}(J/g)$	$T_{IN}(K)$	S_{IN}	$a(J/gK)$
0	2.1	313.6	0.34	0.1159
0.099	2.2013	314.73	0.2483	0.2269
0.179	2.2866	315.15	0.2463	0.2392
0.199	2.3382	316.04	0.2452	0.1418
0.300	2.5980	316.77	0.2535	0.2553
0.330	2.7062	317.17	0.2365	0.3050
0.400	2.9150	317.32	0.2559	0.2805
0.430	2.9150	317.75	0.2287	0.3508
0.499	3.3441	318.70	0.2284	0.4022
0.569	3.6900	319.65	0.2444	0.3866
0.629	4.0510	319.63	0.2613	0.3711

III. EXPERIMENTAL

The LC compounds 8CB and 10CB were purchased from AWAT Co. Ltd, Poland (with purity of 99.8%, via chromatography), and they were used as received. 8CB-10CB binary mixtures were prepared at room temperature by weighing the pure compounds in the selected proportions. We have prepared 13 different mixtures with mole fractions x of 10CB in the mixtures 0.099, 0.179, 0.199, 0.300, 0.330, 0.400, 0.430, 0.499, 0.569, 0.629, 0.699, 0.749, and 0.800. The pure compounds were first mixed and then heated slightly up to the isotropic phase. Finally, they were annealed for a duration of several days to ensure homogenous mixing.

High-resolution optical birefringence measurements were performed via the rotating analyzer method, details of which can be found elsewhere [37–40]. In this method, light at a wavelength of 633 nm from a laser module passes successively through a polarizer (Thorlabs Inc.), a planar-oriented sample, a quarter-wave plate (Thorlabs), and a rotating Polaroid plate (Knight Optical) with angular frequency ω before reaching a photodiode. The polarizer and the quarter-wave plate are both oriented at an angle of 45° relative to the optical axis of the sample. A reference beam from another laser module passes through the rotating Polaroid plate onto another photodiode. This method allows one to measure the phase angle changes, with respect to the reference beam, with an accuracy of 10^{-4} rad with the help of a lock-in detector (Stanford Research, SR830). In our setup, for a 20 μm thick sample, sensitivity

in the birefringence, Δn of 10^{-6}, is achieved. Temperature was measured and controlled by an RTD sensor (Omega Eng. Corp.) and a Lake Shore Model 331 temperature controller with a resolution and measured stability of 0.001 K. It must be emphasized here that during data acquisition the temperature step was 4 mK and the waiting times were always larger than 60 s until the temperature stability was reached. The whole setup is fully computer controlled via LabVIEW (National Instruments) software. The properly aligned samples were realized separately in commercially manufactured sandwich-type LC cells (Instec Inc.) filled by capillary suction in the isotropic liquid phase of LCs. After the filling process all cells were finally sealed with epoxy sealant. Further details on alignment and cell thickness tests can be found elsewhere [25]. Notice that Δn measurements were performed for several heating and cooling runs, and reproducible results were obtained. In this work, we present Δn data upon cooling for all mixtures.

IV. RESULTS AND DISCUSSION

A. The Halperin-Lubensky-Ma effect

It is well known that while both pure 8CB and 10CB LC compounds exhibit Sm*A* mesophase, namely, partially bilayer smectic, 10CB itself does not display the nematic mesophase. Depicted in Fig. 1 is the experimental (partial) phase diagram of the binary mixtures $8CB_{1-x}10CB_x$ ($0 \leqslant x \leqslant 1$) as a function of the mole fraction x of 10CB based on the optical birefringence measurements. In Fig. 1 we also plot the transition temperatures extracted from calorimetric data [14]. It must be stressed that all phase transition temperatures are in good agreement with the ones reported by Marynissen *et al.* [14]. As seen from Fig. 1, while both the *N*-*I* and *N*-Sm*A* transition temperatures increase with increasing mole fraction x of 10CB, the width of the nematic range decreases substantially. Also, for the mixtures with $x > 0.63$ only the *I*-Sm*A* phase transition is observed as temperature is lowered [14,41]. In this work, in order to test the universal scaling (crossover) form [Eq. (8)] we have particularly focused on the region $0 \leqslant x \leqslant 0.63$ where the *I*-*N*-Sm*A* phase sequence is observed. As stated above, for pure 8CB the *N*-Sm*A* transition has been shown to be continuous within experimental resolution, but consistent with the possibility of the very small latent heat expected from the HLM theory [5,12–15,20–22]. For both pure 10CB and the mixtures with $x > 0.63$, the *I*-Sm*A* transition is first order [14,41]. The optical birefringence of the binary mixtures $8CB_{1-x}10CB_x$ ($0 \leqslant x \leqslant 1$) have been measured in the temperature interval $30\,^{\circ}\mathrm{C} \leqslant T \leqslant 60\,^{\circ}\mathrm{C}$. Data were collected upon cooling from the isotropic liquid phase with an average temperature scanning rate of 1.8 mK/min. In Figs. 2(a)–2(b) optical birefringence Δn data are presented as a function of temperature T for the binary mixtures which exhibit the *I*-*N*-Sm*A* phase sequence together with that of pure 8CB. In the isotropic liquid phase the birefringence is zero, signaling that no measurable pretransitional effects are present in the isotropic phase. Thus the T_{IN} transition temperatures (presented in Fig. 1) were considered to be the lowest temperature corresponding to zero birefringence in the isotropic liquid phase. Similarly, the *I*-Sm*A* transition temperature T_{IA} for pure 10CB and for the mixtures with $x > 0.63$ is assumed to be the lowest temperature corresponding to zero birefringence in the isotropic phase as well. As temperature decreases, the improvement in the average molecular alignment results in a gradual increase seen in Δn. Furthermore, for the mixtures $0 \leqslant x \leqslant 0.629$ (see Fig. 2) upon lowering temperature towards the SmA phase a discernible increase in Δn, thus also in

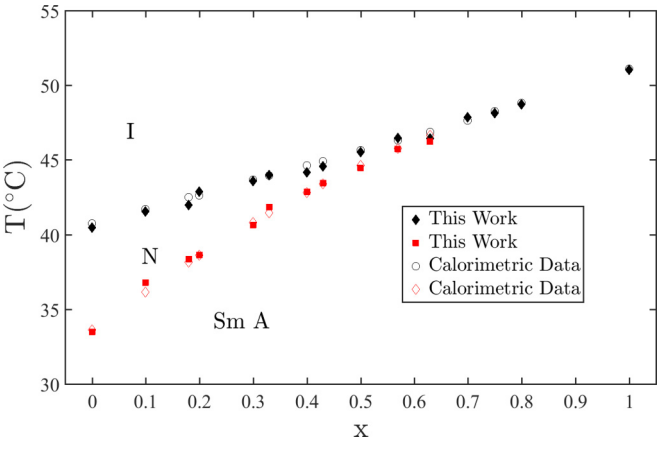

FIG. 1. Partial phase diagram of 8CB-10CB binary mixtures as a function of mole fraction x of 10CB. *I:* isotropic phase, *N:* nematic phase, *SmA*: smectic-*A* phase. Notice that the solid symbols are the optical birefringence data, and the open symbols refer to the calorimetric data from Ref. [14]. For pure 8CB the *N*-*I* and *N*-Sm*A* transition temperatures, extracted from $\Delta n(T)$ data, are from Ref. [35].

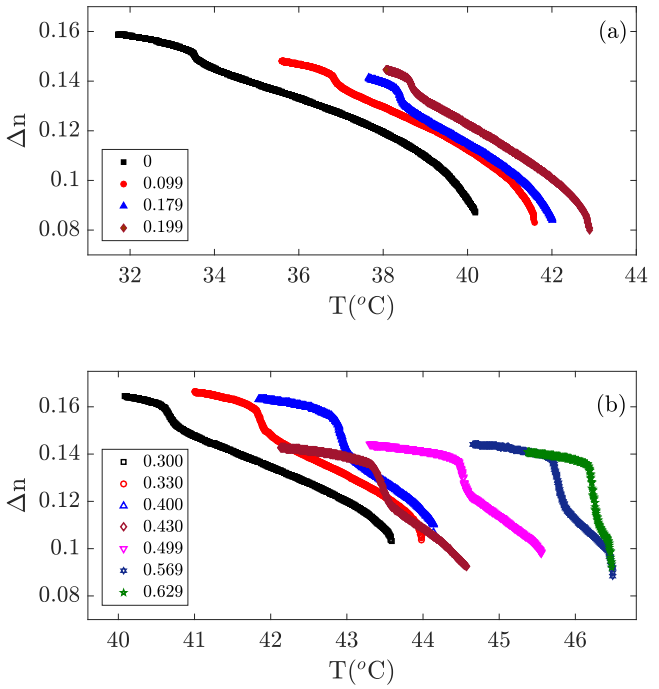

FIG. 2. Temperature dependence of the measured birefringence Δn for the binary mixtures $8CB_{1-x}10CB_x$, with x mole fraction of 10CB. (a) $x = 0$, pure 8CB, from Ref. [35], $x = 0.099$, 0.179, and 0.199, (b) $x = 0.300$, 0.330, 0.400, 0.430, 0.499, 0.569, and 0.629. Different mole fractions x of 10CB are given.

$S(T)$, occurs due to the buildup of the smectic-like short-range order [1]. That increase in the nematic order parameter $S(T)$ can be associated with a better packing of the molecules, due to the onset of the smectic layering and an associated density effect. Thus, one infers that there should be an anomalous increase in the quantity $-d(\Delta n)/dT$ in the immediate vicinity of the N-SmA transition. By following the literature [42,43] the N-SmA transition temperatures T_{NA} presented in the phase diagram (Fig. 1) have been determined from the extrema of the $-d(\Delta n)/dT$ versus T data. For pure 8CB and for the mixtures $x = 0.099$, 0.179, 0.199, 0.300, 0.330, 0.400, 0.430, 0.499, 0.569, and 0.629, pretransitional smectic behavior in $\Delta n(T)$ data have clearly been observed above and below T_{NA}.

In order to obtain the order parameter $S(T)$ from $\Delta n(T)$ via Eq. (5), first we have performed fits using the relation given in Eq. (4) with the fit parameters Δn_0, S^{**}, T^{**}, and β. For the fitting procedure we have used a nonlinear multiparameter fitting program, a subroutine of MATLAB, which has proven to be very efficient [25,31,32,35]. The procedure is based on the conjugated gradient method, details of which can be found elsewhere [31]. The average value of the critical exponent β, describing the limiting behavior of the order parameter $S(T)$ near the N-I transition, has been found to be 0.245 ± 0.002. Together with the fact that Δn has a finite jump at T_{IN}, the value of the exponent β seems to be in line with the tricritical nature of the N-I transition as first proposed by Keyes and Anisimov *et al.* [44,45] and subsequently shown by many others [25,27–33,46]. No further details on the N-I transition will be given since the HLM theory and the critical behavior of the nematic order parameter $S(T)$ near T_{NA} are our primary focus in this work.

As discussed in Sec. I, the HLM theory, which claims that the N-SmA transition is weakly first order in nature, is now well established on the basis of the calorimetric investigations [5,12,15,20,21,23]. This means that a quite small discontinuity in the nematic order parameter $S(T)$ at T_{NA}, namely, $\Delta S_{NA}(T_{NA}) = S_A - S_N$, should be expected. On the other hand, it is not experimentally possible, due to finite resolution, to demonstrate whether $\Delta S_{NA}(T_{NA})$ is absolutely zero (second-order transition) or not. Nevertheless, based on the resolution of the experimental data, one can set an upper limit for $\Delta S_{NA}(T_{NA})$ as was previously done for pure 8CB [22]. As pointed out in our recent work [22], the crucial point is not only the precision in the order parameter $S(T)$ but also the resolution and stability of the temperature readings during the experiment, and the number of points around the transition of interest. Thus in Ref. [22] for pure 8CB, from the detailed inspection of $S(T)$ data near T_{NA} we have arrived at the upper limit of $\Delta S_{NA} \leqslant 0.0002$, corresponding to the reduced entropy difference $\bar{s} = \Delta\bar{S}/R = 4.2 \times 10^{-4}$, which is itself in good agreement with ASC measurements and the HLM theory, namely, $\bar{s} = 1.6 \times 10^{-4}$. By following the strategy given in Ref. [22], in this work, we arrived at values for discontinuities of ΔS_{NA} or in some cases an upper limit of ΔS_{NA} for each mixture of interest from a detailed inspection of $S(T)$ data near T_{NA}. With the help of Eq. (10) we then obtained the corresponding reduced entropy discontinuity. We want to point out here that in deriving the reduced entropy we have used in Eq. (11) the latent heat values, ΔH_{IN}, extracted from ASC data [14] to calculate the parameter a needed in Eq. (10).

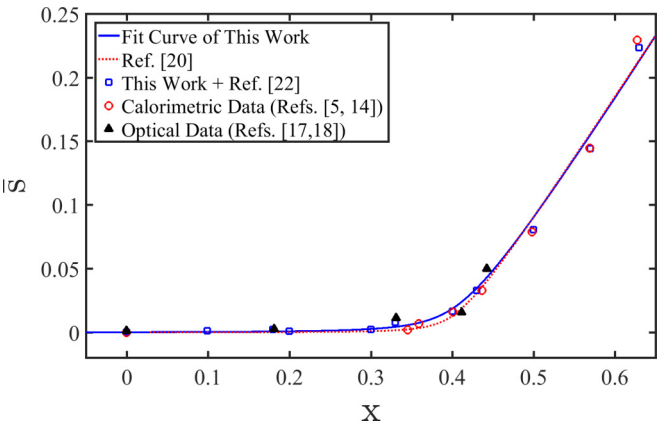

FIG. 3. The derived reduced entropy discontinuity $\bar{s} = \frac{\Delta\bar{S}}{R}$ (R being the gas constant) vs mole fraction x of 10CB fitted to the universal scaling function of Eq. (8) to extract x^* and $\bar{s}^* = \frac{\Delta\bar{S}^*}{R}$ of the LTP.

Figure 3 displays the derived reduced entropy discontinuity $\bar{s} = \Delta\bar{S}/R$ as a function of the mole fraction of 10CB for the binary mixtures $8CB_{1-x}10CB_x$, exhibiting the N-SmA transition. However, as for pure 8CB [22] for the three lowest concentrations ($x = 0.099$, 0.179, and 0.199) it was possible only to arrive at upper limits indicated with thin vertical lines (see Figs. 4 and 5). In Table II the parameter values extracted from different fits of $\bar{s} = \Delta\bar{S}/R$ with Eq. (8) are tabulated. In the fit only birefringenge data with clear discontinuities (excluding pure 8CB and the mole fractions $x = 0.099$, 0.179, and 0.199) were fitted. In Table I we also give the previously published values of the fit parameters derived from calorimetry [20,21] and capillary-length measurements [24]. Also, in Fig. 3 the reduced entropy discontinuity $\bar{s} = \Delta\bar{S}/R$ values from calorimetric data [14] are plotted as well as the results of Yethiraj *et al.* [17,18]. It is useful pointing out that while for the mixtures $x < 0.300$ no calorimetric data are available (Fig. 3 in Ref. [14]), the agreement is excellent for the mixtures $x \geqslant 0.300$. We note, however, that from closer looking at Fig. 3 $\bar{s}$ values for the mixtures $0.099 \leqslant x \leqslant 0.199$ seem to be larger than the HLM curve. To get a closer look, we plot in Fig. 4 in

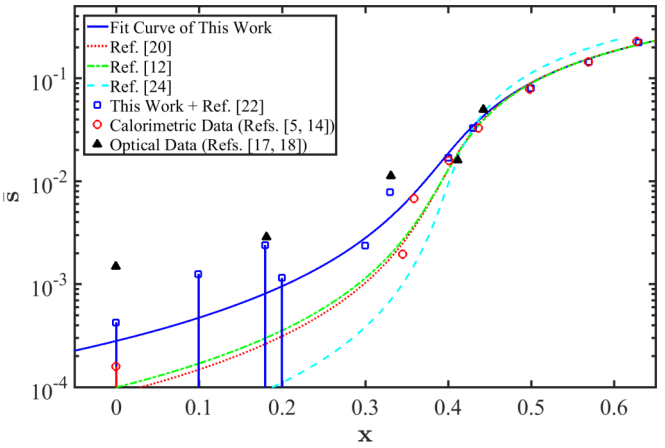

FIG. 4. The reduced entropy discontinuity $\bar{s}$ of Fig. 3 vs the mole fraction x of 10CB on a semilogarithmic scale. Different lines represent fits with different data sets as indicated.

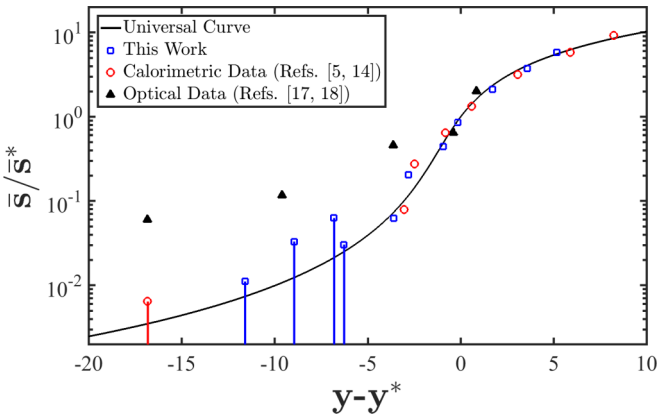

FIG. 5. Comparison in a semilogarithmic plot of the different data sets with the universal curve resulting from Eq. (8).

a semilogarithmic scale $\bar{s}$ as a function of the mole fraction x since then the low $\bar{s}$ side is more clearly visible. For comparison purposes we also display the fitting curves with the literature parameters given in Table I. From Fig. 4 it can be concluded that, within the experimental accuracy, our data are consistent with the shape of the HLM curve. It is also clear that there are differences between the fitting curves based on different types of data sets. It can also be seen that the shape of the fitting curve is to a large extend determined by the more accurate values at the higher x values. It should also be obvious that the HLM $x = 0$ value is substantially lower than the value of Yethiraj *et al.* [18] but consistent with the upper limit from calorimetry and our upper limit from birefringence measurements. As pointed out above, experimental data can be compared with a universal scaling function given by Eq. (8). Such a comparison is made in Fig. 5 for our birefringence results and with different literature data. There is good consistency with the HLM curve, except for the known deviations of the low mole fraction data of Yethiraj *et al.* [18].

B. Pretransitional behavior

It is a well-known fact that in liquid crystalline materials exhibiting the Sm*A* phase as well as the *N* phase the mutual coupling between the nematic and the Sm*A* order parameters manifests itself by an enhancement in the nematic (orientational) order parameter $S(T)$, thus, also in the birefringence $\Delta n(T)$. For this enhancement the relationship, in the mean-field approach, $S - S_0 = C_c \chi \langle |\Psi|^2 \rangle$ was postulated by taking into account the short-range smectic ordering fluctuations in the *N* phase [8,38]. Here S_0 refers to the hypothetical nematic order parameter in the absence of any smectic ordering, C_c is a coupling constant, and χ is a response function, depending on the degree of the saturation of the *N* phase. Additionally, based on a consequence of the Landau-de Gennes free energy [8,47,48], it is straightforward to obtain the following expression:

$$\langle |\Psi|^2 \rangle = U + V_{\pm} |t|^{\lambda}, \tag{12}$$

where $t = (T - T_{NA})/T_{NA}$, and $\lambda = 1 - \alpha$, with α the specific heat capacity exponent. The plus-minus sign stands for above and below the *N*-Sm*A* transition temperature T_{NA}, respectively. Since in the *N* and Sm*A* phases, Δn and S are proportional to each other [see Eq. (5)], our high-resolution $\Delta n(T)$ data have been used to extract the exponent λ in Eq. (12) in the vicinity of the *N*-Sm*A* transition. Particularly noteworthy is the fact that one can infer the relationship $\lambda = 1 - \alpha$ with the help of the Lorenz-Lorentz relation between the refractive index and the density. In fact, when going from the *N* phase to the Sm *A* phase the increase in $\Delta n(T)$, and thus in $S(T)$, is accompanied by a similar increase in the density upon lowering the temperature [49,50]. Hence, on the basis of the generalized Pippard relations, the critical variation of both the density and the isobaric volume thermal-expansion coefficient with temperature are expected to exhibit the same power law divergence as that of the specific heat capacity with the critical exponent α [49–51].

In an attempt to look in detail at the critical behavior of the nematic order parameter $S(T)$ near the *N*-Sm*A* transition, one can use the quantities $-dS/dT$ or $-d(\Delta n)/dT$. Notice that for both cases a diverging critical behavior should be observed. For the latter quantity the limiting critical power law behavior including some linear temperature dependent behavior can be fitted with the following equation:

$$-\frac{d(\Delta n)}{dT} = A_n^{\pm} \left| 1 - \frac{T}{T_{NA}} \right|^{-\alpha} + B_n + C_n T + E_n T^2, \tag{13}$$

where $\pm$ indicates above and below the transition.

As was discussed in our previous works [22,25,32], the local slope $-d(\Delta n)/dT$ has been shown to exhibit substantial scatter if one only uses consecutive closely spaced (here typically 4 mK) data points. However, substantial reduction of the scatter is obtained by local linear fits of an appropriate chosen number of data points, by progressing along the curve by adding a data point at higher temperature and leaving out the lowest one in the previous linear fit. Subsequently we argued that [22,25,32] a substantial reduction in scatter can be obtained by defining a new quotient such that

$$Q(T) = -\frac{\Delta n(T) - \Delta n(T_{NA})}{T - T_{NA}}. \tag{14}$$

It corresponds to the slope of the chord connecting $\Delta n(T)$ at T with $\Delta n(T_{NA})$ at T_{NA}. We may emphasize here that the quotient $Q(T)$ is similar to the quantity $C_{\text{cal}}(T) = [H(T) - H_C]/(T - T_C)$, with $H(T)$ the temperature-dependent enthalpy obtained by ASC [5,7,52]. It has been well established that [5,22] like the correspondence between $C_{\text{cal}}(T)$ and the specific heat capacity $C_P = dH/dT$, $Q(T)$ and $-d(\Delta n)/dT$ exhibit the same power-law behavior with the same critical exponent α and the background term but, with a different critical amplitude, modified by a factor of $(1 - \alpha)^{-1}$. As we discussed in detail in our previous works [25,32], the

TABLE II. Parameter values obtained from the fitting of the reduced entropy discontinuity near the *N*-Sm*A* transition with Eq. (8) in the binary mixtures $8CB_{1-x}10CB_x$.

x^*	$\bar{s}^*$	$\hat{a}$	Ref.
0.4352	0.03803	1.0130	This work
0.4213	0.02467	0.9860	[20, 21]
0.416	0.020	1.24	[24]
0.4243	0.0261	0.993	[12]

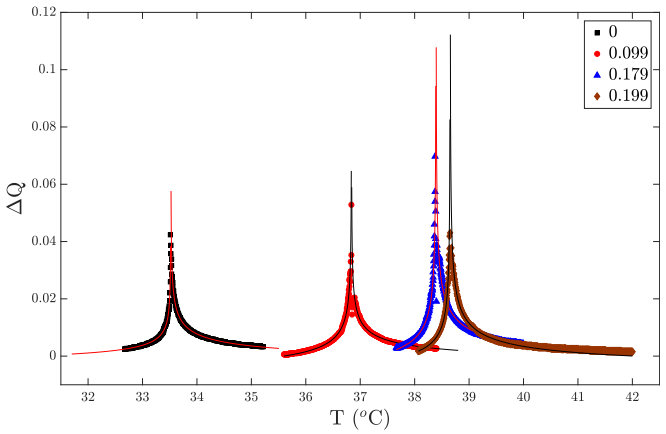

FIG. 6. Temperature behavior of the quotient $\Delta Q(T)$ in the vicinity of the N-SmA transition for the binary mixtures $0.099 \leqslant x \leqslant 0.199$ together with pure 8CB. Solid lines are the fits to Eq. (15). The different mole fractions of 10CB are indicated in the figure.

quotient $Q(T)$ has a regular background contribution resulting from the regular temperature dependence of nematic order parameter. This background can be obtained by extending the fit performed with Eq. (4) in the nematic range to lower temperatures in the Sm A phase and introducing the so-called background quotient $Q_b(T) = -[\Delta n_{\rm fit}(T) - \Delta n_{\rm fit}(T_{NA})]/(T - T_{NA})$. Thus, near the N-SmA transition the critical anomaly in the quotient $\Delta Q(T) = Q(T) - Q_b(T)$ can be observed more clearly, as depicted in Fig. 6 for the binary mixtures with $x \leqslant 0.199$, which can experimentally be considered to be nearly second order. In Fig. 6 we present an overview of the temperature dependence of the quotient $\Delta Q(T)$ in the immediate vicinity of T_{NA} for those mixtures as well as for pure 8CB. In Fig. 6, for pure 8CB, the quotient $\Delta Q(T)$ has been calculated from the birefringence data given in Ref. [35]. It should be underlined here that the peak height values of the quotient $\Delta Q(T)$ near T_{NA} increase substantially with increasing mole fraction of 10CB, namely, with decreasing the nematic range. This behavior is indicative of the increasing strength of the coupling between the nematic and smectic-A order parameters. Also, a clear increase in the $\Delta Q(T)$ wings on both sides of T_{NA} with increasing x can be noted. Additionally, in order to shed light on the critical anomaly presented in Fig. 6, the $\Delta Q(T)$ data have been

TABLE III. Results of the fits to Eq. (15) for the binary mixtures $8CB_{1-x}10CB_x$ for which, within experimental resolution, a second-order N-SmA transition is observed.

x	Phase	α	A_Q^+, A_Q^-	B_Q
0	N	0.3184 ± 0.0050	0.0018 ± 0.0007	-0.0061 ± 0.0002
	SmA	0.3183 ± 0.0050	0.0012 ± 0.0002	-0.0055 ± 0.0005
0.099	N	0.3383 ± 0.0018	0.0014 ± 0.0001	-0.0060 ± 0.0001
	SmA	0.3384 ± 0.0020	0.0017 ± 0.0005	-0.0108 ± 0.0006
0.179	N	0.3819 ± 0.0019	0.0016 ± 0.0002	-0.0074 ± 0.0006
	SmA	0.3820 ± 0.0014	0.0014 ± 0.0002	-0.0124 ± 0.0006
0.199	N	0.4146 ± 0.0038	0.0011 ± 0.0002	-0.0073 ± 0.0003
	SmA	0.4142 ± 0.0020	0.0009 ± 0.0003	-0.0100 ± 0.0004

analyzed with the following fitting expression:

$$\Delta Q(T) = A_Q^{\pm}\left|1 - \frac{T}{T_{NA}}\right|^{-\alpha} + B_Q + C_Q T. \qquad (15)$$

Here $A_Q^{\pm}$ are the critical amplitudes, and $(B_Q + C_Q T)$ is the background contribution. Notice that during the $\Delta Q(T)$ data fitting to Eq. (15) we have imposed $C_Q = 0$ and fixed T_{NA} for each mixture at the values given in Fig. 1. The quality of the fits, on both sides of the transition temperature T_{NA}, has been tested by evaluating the reduced error function χ_v^2, the definition of which can be found elsewhere [25,31,53]. Further, we have tested the stability of the fit results by a range shrinking method in which the points situated at the ends of the $\Delta Q(T)$ data set were gradually discarded and the data refitted [25,31]. Also, we notice that the inclusion of correction-to-scaling terms, namely, $D_{\pm}|t|^{\Delta}$ terms above and below T_{NA} with $\Delta \approx 0.5$, did not improve the fit quality appreciably. The fits to Eq. (15) are displayed as solid lines in Fig. 6, while the corresponding fit values are compiled in Table III. From Table III it should be clear that, for the four concentrations analyzed, the value of the critical exponent α is, within experimental uncertainty, the same above and below the N-SmA transition. In Table IV results of similar fits with Eq. (13) for $-d(\Delta n)/dT$ are summarized. Full consistency with the α values in Table III can be observed.

For the mixtures at higher concentrations where clear discontinuities in Δn have been observed, it is not possible anymore to impose the same transition temperature for the data above and below the transition. Instead of T_{NA} in Eq. (13),

TABLE IV. Results of the fits to Eq. (13) for $-d(\Delta n)/dT$ data of the binary mixtures $8CB_{1-x}10CB_x$ for which, within experimental resolution, a second-order N-SmA transition is observed.

x	Phase	α	A_n^+, A_n^-	C_n	B_n
0	N	0.3247 ± 0.0063	0.0011 ± 0.0001	0.0012 ± 0.0007	-0.3699 ± 0.0022
	SmA	0.3178 ± 0.0012	0.0008 ± 0.0001	0.0003 ± 0.00004	-0.1070 ± 0.0010
0.099	N	0.3493 ± 0.0013	0.0010 ± 0.0005	$8.9 \times 10^{-6} \pm 2.4 \times 10^{-7}$	-0.0037 ± 0.0007
	SmA	0.3471 ± 0.0015	0.0009 ± 0.00007	$8.9 \times 10^{-6} \pm 2.4 \times 10^{-7}$	-0.0060 ± 0.0007
0.179	N	0.392 ± 0.009	0.0013 ± 0.0003	0.00012 ± 0.00007	-0.0460 ± 0.0073
	SmA	0.392 ± 0.005	0.0007 ± 0.0002	$4.3 \times 10^{-5} \pm 1.1 \times 10^{-6}$	-0.0177 ± 0.0030
0.199	N	0.4224 ± 0.0034	0.0006 ± 0.0002	0.0007 ± 0.00002	-0.2194 ± 0.0030
	SmA	0.4252 ± 0.0037	0.0006 ± 0.0002	$2.8 \times 10^{-6} \pm 3.6 \times 10^{-7}$	-0.0049 ± 0.0016

TABLE V. Results of the fits for $8CB_{1-x}10CB_x$ binary mixtures exhibiting a clear discontinuity in Δn data near the *N*-Sm*A* transition [see Eq. (13); notice that instead of T_{NA} separate T_1 parameters above and below the transition are introduced].

x	Phase	α	T_1(°C)	A_n^+, A_n^-	C_n	B_n	E_n
0.300	*N*	0.5098 ± 0.0220	40.660 ± 0.011	0.0007 ± 0.0001	−1.0765 ± 0.0120	166.942 ± 0.097	0.0017 ± 0.0001
	Sm*A*	0.5039 ± 0.0600	40.678 ± 0.043	0.0009 ± 0.0002	−1.0657 ± 0.0160	171.614 ± 0.090	0.0017 ± 0.0001
0.330	*N*	0.4867 ± 0.0110	41.849 ± 0.068	0.0010 ± 0.0003	−1.0171 ± 0.0040	157.960 ± 0.230	0.0016 ± 0.0005
	Sm*A*	0.4891 ± 0.0160	41.892 ± 0.062	0.0016 ± 0.0004	−1.0800 ± 0.0054	175.137 ± 0.290	0.0017 ± 0.0003
0.400	*N*	0.5173 ± 0.0410	42.894 ± 0.091	0.0017 ± 0.0008	−2.5535 ± 0.0020	397.033 ± 0.250	0.0041 ± 0.0003
	Sm*A*	0.4962 ± 0.0090	42.940 ± 0.090	0.0013 ± 0.0007	−1.0658 ± 0.0010	170.056 ± 0.850	0.0017 ± 0.0005
0.430	*N*	0.5283 ± 0.0090	43.463 ± 0.052	0.0012 ± 0.0001	−1.1465 ± 0.0910	173.492 ± 0.190	0.0019 ± 0.0006
	Sm*A*	0.4852 ± 0.0500	43.506 ± 0.032	0.0024 ± 0.0001	−0.9008 ± 0.0310	146.353 ± 0.310	0.0014 ± 0.0002
0.499	*N*	0.4990 ± 0.0440	44.501 ± 0.055	0.0019 ± 0.0006	−2.5659 ± 0.0025	397.690 ± 0.410	0.0014 ± 0.0003
	Sm*A*	0.5095 ± 0.0640	44.520 ± 0.033	0.0011 ± 0.0005	−0.8981 ± 0.0016	146.124 ± 0.085	0.0013 ± 0.0002

we introduced T_1 which could assume a different value for the data below and above the transition, in much the same way for the first-order nematic-isotropic transition. Table V summarizes the fit results for the mole fractions 0.30, 0.33, 0.40, 0.43, and 0.499. For the mole fractions of 0.569 and 0.629 the pretransitional contributions were too small to arrive at reliable fitting results. Figure 7 gives the 10CB mole fraction, x dependence of the effective critical exponent α (average value from below and above T_{NA}), and the derived reduced entropy discontinuity $\bar{s} = \Delta\bar{S}/R$, which is itself proportional to the latent heat, for the investigated binary mixtures and as well as for pure 8CB. By inspection of Fig. 7 together with Tables III and IV, it is observed that the critical exponent α reaches its tricritical value $\alpha_{\mathrm{TCP}} = 0.5$ for the 10CB mole fraction of $x = 0.330$ and, within our experimental resolution, nearly zero latent heats (entropy discontinuities) are observed for the α values smaller than the TCP value. This behavior is in good accordance with the ones by ASC measurements [14]. It can be noted that, within the experimental uncertainity, the values of the effective exponent α seem quite close to TCP value for the mixtures $0.330 \leqslant x \leqslant 0.629$.

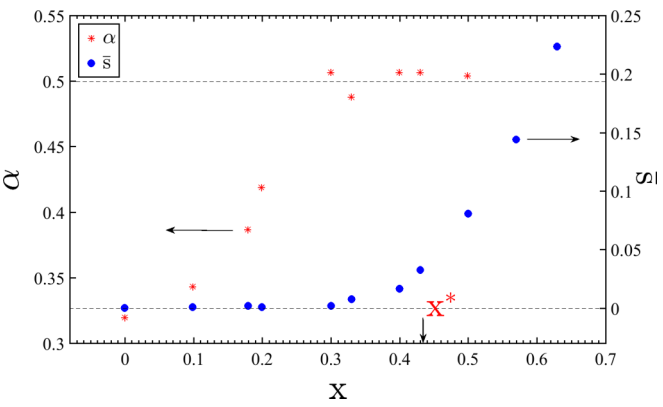

FIG. 7. The x dependence of the effective critical exponent α (asterisks), and the reduced entropy discontinuity $\bar{s}$ (solid circles) for the binary mixtures $8CB_{1-x}10CB_x$. Here x^* refers to the mole fraction of the Landau tricritical point (see text).

V. SUMMARY AND CONCLUSION

Presented in this work are high-resolution experimental data for the temperature dependence of the optical birefringence of the binary mixtures $8CB_{1-x}10CB_x$ by using a rotating analyzer method. The *N-I*, *N*-Sm*A*, and *I*-Sm*A* transititons have been clearly identified from the birefringence data. The birefringence data have then been used to probe the temperature behavior of the nematic order parameter S [22,25,31,32,35]. Particular emphasis has been devoted to the derived nematic order parameter values along the *N*-Sm*A* phase transition line of the phase diagram of the binary system. From the detailed inspection of $S(T)$ data across T_{NA} we then obtained the corresponding reduced entropy discontinuity $\bar{s} = \Delta\bar{S}/R$ at the *N*-Sm*A* transition. For the mixtures with $x \geqslant 0.30$ we found $\bar{s}$ values in agreement with the calorimetric data [5,14] and with the optical data of Yethiraj *et al.* [17,18]. However, for the $\bar{s}$ values of the mixtures $x = 0.099, 0.179$, and 0.199 we could obtain only upper limits for possible discontinuities. These values indicated by the data point symbols with thin vertical lines in Figs. 4 and 5. For these mixtures the upper limits are larger than the value obtained for pure 8CB and lower than the discontinuities reported in Refs. [17] and [18], but not substantially. Our derived reduced entropy discontinuity values for $x \geqslant 0.30$ could be well fitted with the universal crossover form (universal scaling form) of Eq. (8) consistent with the HLM theory [10], albeit with some differences in parameters (see Table I) in comparison with similar fits in Refs. [12], [20], and [24]. This results in some differences between the fitting curves below $x = 0.30$, as presented in Fig. 4. However, using the corresponding parameter values given in Table I for the calorimetry and birefringence data sets gives excellent correspondance with the universal curve, as displayed in Fig. 5. The reduced entropy ($\bar{s}$) from Refs. [17] and [18], plotted with the parameters given in Ref. [12] (as done in Refs. [17,18]), clearly deviates from the universal curve. In an effort to further test the HLM conjecture and improve the agreement between calorimetry and our optical technique, a study of the binary mixtures of octyloxycyanobiphenyl (8OCB) and nonyloxycyanobiphenyl (9OCB) LCs is in progress and will be presented elsewhere.

By exploiting the fact that the temperature derivative of the order parameter $S(T)$ near T_{NA} exhibits the same power

law divergence as the specific heat capacity [22,27–30,32], we have extracted the effective critical exponent values for the compositions under study. The critical exponent α has been observed to reach the tricritical value $\alpha_{\mathrm{TCP}} = 0.5$ for the 10CB mole fraction of $x = 0.330$ and, within our experimental resolution, nearly zero latent heats (or entropy discontinuities) have been noted for the α values smaller than the TCP value. This behavior is in good agreement with those observed by ASC measurements [14]. The extracted values of the effective exponent α seem to be quite close to TCP value for the mixtures $0.330 \leqslant x \leqslant 0.629$ within the experimental uncertainty. Since there is no calorimetric information on the α values for the compositions $x > 0.330$, it is not possible to compare with the exponent values reported here.

ACKNOWLEDGMENTS

We thank Şişe Cam Glass Research Center for the use of SEM. This work was supported by the Research Fund of Istanbul Technical University under Grants No. 37630 and No. 38206.

[1] P. G. de Gennes and J. Prost, *The Physics of Liquid Crystals* (Oxford University Press, Oxford, 1993).
[2] G. Vertogen and W. H. de Jeu, *Thermotropic Liquid Crystal: Fundamentals* (Springer-Verlag, Berlin, 1988).
[3] S. Kumar (ed.), *Liquid Crystals* (Cambridge University Press, Cambridge, 2001).
[4] G. B. Kasting, K. J. Lushington, and C. W. Garland, Phys. Rev. B **22**, 321 (1980).
[5] J. Thoen, H. Marynissen, and W. Van Dael, Phys. Rev. A **26**, 2886 (1982).
[6] C. W. Garland and G. Nounesis, Phys. Rev. E **49**, 2964 (1994) and references cited therein.
[7] J. Thoen, C. Gordoyiannis, and C. Glorieux, Liq. Cryst. **36**, 669 (2009) and references cited therein.
[8] P. G. de Gennes, Mol. Cryst. Liq. Cryst. **21**, 49 (1973).
[9] K. Kobayashi, Phys. Lett. A **31**, 125 (1970); W. L. McMillan, Phys. Rev. A **4**, 1238 (1971).
[10] B. I. Halperin, T. C. Lubensky, and S. K. Ma, Phys. Rev. Lett. **32**, 292 (1974); B. I. Halperin and T. C. Lubensky, Solid State Commun. **14**, 997 (1974).
[11] M. A. Anisimov, V. P. Voronov, E. E. Gorodetskii, V. E. Podnek, and F. Kholmurodov, JETP Lett. **45**, 425 (1987).
[12] M. A. Anisimov, P. E. Cladis, E. E. Gorodetskii, D. A. Huse, V. E. Podneks, V. G. Taratuta, W. van Saarloos, and V. P. Voronov, Phys. Rev. A **41**, 6749 (1990).
[13] J. Thoen, H. Marynissen, and W. Van Dael, Phys. Rev. Lett. **52**, 204 (1984).
[14] H. Marynissen, J. Thoen, and W. Van Dael, Mol. Cryst. Liq. Cryst. **124**, 195 (1985).
[15] M. A. Anisimov, V. P. Voronov, A. O. Kulkov, V. N. Petukhov, and F. Kholmurodov, Mol. Cryst. Liq. Cryst. **150 B**, 399 (1987).
[16] A. Yethiraj and J. Bechhoefer, Mol. Cryst. Liq. Cryst. **304**, 301 (1997).
[17] A. Yethiraj and J. Bechhoefer, Phys. Rev. Lett. **84**, 3642 (2000).
[18] A. Yethiraj, R. Mukhopadhyay, and J. Bechhoefer, Phys. Rev. E **65**, 021702 (2002).
[19] I. Lelidis, Phys. Rev. Lett. **86**, 1267 (2001).
[20] G. Cordoyiannis, C. S. P. Tripathi, C. Glorieux, and J. Thoen, Phys. Rev. E **82**, 031707 (2010).
[21] C. S. P. Tripathi, P. Losada-Perez, J. Leys, G. Cordoyiannis, C. Glorieux, and J. Thoen, Eur. Phys. J. E **35**, 54 (2012).
[22] M. C. Çetinkaya, S. Yıldız, H. Özbek, P. Losada-Perez, J. Leys, and J. Thoen, Phys. Rev. E **88**, 042502 (2013).
[23] J. Salud, D. O. Lopez, S. Diez-Berart, and M. R. de la Fuente, Liq. Cryst. **40**, 293 (2013).
[24] N. Tamblyn, P. Oswald, A. Miele, and J. Bechhoefer, Phys. Rev. E **51**, 2223 (1995).
[25] S. Erkan, M. Çetinkaya, S. Yıldız, and H. Özbek, Phys. Rev. E **86**, 041705 (2012).
[26] M. F. Vuks, Opt. Spectrosc. **20**, 361 (1966); S. Chandrasekhar and N. V. Madhsudana, J. Phys. Colloq. **30**, C4-24 (1969).
[27] A. Chakraborty, S. Chakraborty, and M. K. Das, Phys. Rev. E **91**, 032503 (2015).
[28] S. K. Sarkar and M. K. Das, J. Mol. Liq. **199**, 415 (2014).
[29] S. K. Sarkar and M. K. Das, RSC Adv. **4**, 19861 (2014).
[30] S. K. Sarkar, P. C. Barman, and M. K. Das, Physica B **446**, 80 (2014).
[31] I. Chirtoc, M. Chirtoc, C. Glorieux, and J. Thoen, Liq. Cryst. **31**, 229 (2004).
[32] S. Yıldız, H. Özbek, C. Glorieux, and J. Thoen, Liq. Cryst. **34**, 611 (2007).
[33] M. Simoes and D. S. Simeao, Phys. Rev. E **74**, 051701 (2006).
[34] S. Singh, Phys. Rep. **324**, 107 (2000); B. Van Roie, J. Leys, K. Denolf, C. Glorieux, G. Pitsi, and J. Thoen, Phys. Rev. E **72**, 041702 (2005); M. Marinelli and F. Mercuri, *ibid.* **61**, 1616 (2000); P. K. Mukherjee and T. B. Mukherjee, Phys. Rev. B **52**, 9964 (1995).
[35] H. Özbek, Ş. Üstunel, E. Kutlu, and M. C. Çetinkaya, J. Mol. Liq. **199**, 275 (2014).
[36] M. S. Zakerhamidi and H. Rahimzadeh, Mol. Cryst. Liq. Cryst. **569**, 92 (2012); J. Mol. Liq. **172**, 41 (2012); S. S. Sastry, T. V. Kumari, K. Mallika, B. G. S. Rao, S. T. Ha, and S. Lakshminarayana, Liq. Cryst. **39**, 295 (2012).
[37] E. F. Gramsbergen and W. H. de Jeu, J. Chem. Soc., Faraday Trans. 2 **84**, 1015 (1988).
[38] K. C. Lim and J. T. Ho, Phys. Rev. Lett. **40**, 944 (1978).
[39] K. C. Lim and J. T. Ho, Mol. Cryst. Liq. Cryst. **47**, 173 (1978).
[40] D. A. Dunmur, in *Physical Properties of Liquid Crystals: Nematics*, edited by D. A. Dunmur, A. Fukuda, and G. R. Luckhurst (Institution of Electrical Engineers, London, 2002).
[41] H. Marynissen, J. Thoen, and W. Van Dael, Mol. Cryst. Liq. Cryst. **97**, 149 (1983).
[42] A. V. Kityk and P. Huber, Appl. Phys. Lett. **97**, 153124 (2010); S. Calus, B. Jablonska, M. Busch, D. Rau, P. Huber, and A. V. Kityk, Phys. Rev. E **89**, 062501 (2014).
[43] P. Huber, M. Busch, S. Calus, and A. V. Kityk, Phys. Rev. E **87**, 042502 (2013); A. V. Kityk *et al.*, Soft Matter **10**, 4522 (2010).

[44] P. H. Keyes, Phys. Lett. A **67**, 132 (1978).
[45] M. A. Anisimov, S. R. Garber, V. S. Esipov, V. M. Mamnitskii, G. I. Ovodov, L. A. Smolenko, and E. L. Sorkin, JETP **45**, 1042 (1977); M. A. Anisimov, Mol. Cryst. Liq. Cryst. **162A**, 1 (1988), Special Topics XXXI.
[46] D. S. Simeao and M. Simoes, Mol. Cryst. Liq. Cryst. **576**, 88 (2013); M. Simoes, D. S. Simeao, and K. E. Yamaguti, Liq. Cryst. **38**, 935 (2011).
[47] M. E. Fisher and A. Aherony, Phys. Rev. Lett. **31**, 1238 (1973).
[48] K. K. Chan, M. Deutsch, B. M. Ocko, P. S. Pershan, and L. B. Sorensen, Phys. Rev. Lett. **54**, 920 (1985).
[49] A. Zywocinski and S. A. Wieczorek, J. Phys. Chem. B **101**, 6970 (1997).
[50] A. Zywocinski, S. A. Wieczorek, and J. Stecki, Phys. Rev. A **36**, 1901 (1987).
[51] E. Anesta, G. S. Iannacchione, and C. W. Garland, Phys. Rev. E **70**, 041703 (2004) and references cited therein.
[52] J. Thoen, In *Heat Capacities: Liquids, Solutions, and Vapours*, edited by E. Wilhelm and T. M. Letcher (Royal Society of Chemistry, London, 2010).
[53] P. R. Bevington and D. K. Robinson, *Data Reduction and Error Analysis for the Physical Sciences*, 3rd ed. (McGraw Hill, New York, 2003).